

Modeling steady wear of steel/ Al_2O_3 -Al particle reinforced composite system

Zhenfang Zhang, Liangchi Zhang, Yiu-Wing Mai

Centre for Advanced Materials Technology, Department of Mechanical and Mechatronic Engineering, University of Sydney, Sydney, NSW 2006, Australia

Received 4 June 1996; accepted 29 April 1997

Abstract

Considering that harder asperities on one surface would plastically deform the contact areas of a softer counterpart surface, a theoretical model has been developed to describe the steady sliding wear in a system of an alumina particle reinforced aluminium metal matrix composite pin on a steel disk. The model predicts that the volumetric wear of the pin-on-disk system is proportional to the applied load, and depends on the particle volume fraction of the composite and the relative hardness of the rubbing pair. Experimental results obtained from the steady wear of a particulate Al_2O_3 -6061 Al composite/carbon steel system are in reasonably good agreement with theoretical predictions. However, many more experimental data are needed to confirm the general applicability of the proposed wear model for metal matrix composites. © 1997 Elsevier Science S.A.

Keywords: MMC composite; Rubbing pairs; Steady wear; Plastic deformation; Modeling

1. Introduction

Previous studies have shown that during steady wear in a wear system composed of steel and aluminum matrix reinforced with ceramic particles, the friction coefficient, wear rate, types of wear debris and wear surface topography are all relatively constant with time, and the wear mechanisms in this regime are dominated by mild adhesion and abrasion [1–7]. In such a system, both the steel and composite would be mutually worn because both rubbing surfaces possess relatively hard asperities. Although ceramic particle-reinforced aluminum alloys can offer better wear resistance, they cause significant wear on the counterpart surface thus limiting their applications. Understanding the key factors of wear and seeking a better metal matrix composite material (MMC) and rubbing pair have therefore been recent major issues of research. To elucidate the steady wear mechanisms of MMCs, extensive studies have been carried out by previous researchers [1–5,7], and it is shown that the steady wear of a system is caused by strain accumulation at the wearing surfaces. However, quantitative models to predict wear in this regime are few. The purpose of this paper is to develop a new steady wear model based on relevant wear mechanisms and existing asperity contact models.

The linear wear law of Archard [8] and the abrasive wear law of Khurshov [9] have led to significant progress in eval-

uating wear rates quantitatively. Archard [8] assumed that the contact process consisted of the making and breaking of junctions, and that the real contact area of the contacting surfaces is the sum of the areas of all junctions. Thus a well-known wear equation was given in the form:

$$V = K \frac{PL}{H} \quad (1)$$

where V is the wear volume, P is the total normal load L is the sliding distance, H is the flow pressure or hardness of the material and K is the wear coefficient. The wear coefficient K , which is interpreted as the probability of an interacting asperity giving rise to a wear particle, is influenced by elastic or plastic deformation, surface roughness and some material properties. This model is based on the assumption that wear only occurs at the soft surface, the deformation of which is entirely plastic and the wear particle is hemispherical in shape. This assumption is oversimplified because the contact area must consist of both elastic and plastic deformations. Nevertheless, many researchers arrived at the same form of wear equation working from different points of view [9–11].

It has been argued that all asperities in contact support loads elastically and plastically, but only those plastically deformed asperities cause wear [12]. With simplified but appropriate assumptions, Finkin [12] obtained a linear law of wear by considering the formation of a wear particle using

a fatigue failure criterion of strain ratio and a probabilistic treatment of height distribution and surface contact. Halling [13] also introduced Greenwood and Williamson's probabilistic treatment of asperity contact [14] and assumed that both elastic and plastic asperity interactions contributed to wear in accordance with a strain ratio fatigue failure law, essentially the same as Archard's Eq. (1). Generally, Archard's classical linear wear equation is valid for most metals sliding in steady state and is applicable to describe the system wear of a MMC/steel system if hard asperities exist on each surface.

2. Theory

The above discussion shows that for a system with a MMC pin and a steel disk, steady wear occurs on both surfaces and is caused by plastic deformation of contact asperities. Investigations [2,7] showed that the hard particles on the composite surface were removed at random by fracturing and debonding during sliding in steady wear. But statistically the percentage of the hard asperities on the composite surface remains unchanged, since the particles immediately beneath the contact surface would be exposed when the top layer was removed gradually. The particle distribution in a composite of 20% Al₂O₃-Al composite with an average particle diameter of 8.8 μm is shown in Fig. 1. It is noted that the particle distribution in any cross section remains similar to that shown in this micrograph.

Clearly, in the steady wear regime, the volumetric wear of a given rubbing pair is proportional to the sliding distance and the applied load that causes plastic deformation [15]. Therefore, Archard's equation can be applied to both the steel and MMC surfaces. This brings about

$$V_1 = K_1 \frac{P_1 L}{H_1} \tag{2}$$

for the MMC pin and,

$$V_2 = K_2 \frac{P_2 L}{H_2} \tag{3}$$

for the steel disk. The systems wear, *V*, is thus a summation of *V*₁ and *V*₂, i.e.

$$V = L \left(\frac{K_1 P_1}{H_1} + \frac{K_2 P_2}{H_2} \right) \tag{4}$$

where *P*₁ and *P*₂ are the loads which cause wear on the surfaces 1 and 2, (see Fig. 2), *L* is the sliding distance, *H*₁ and *H*₂ are the hardness of the MMC and steel, respectively.

The real contact area, together with the deformed and non-deformed areas on the composite pin is illustrated in Fig. 3. The total deformed area on surface 1 is: *A*₁ = *A*₁₁ + *A*₁₂ + ... + *A*_{1i}; similarly, the total deformed area on surface 2 is: *A*₂ = *A*₂₁ + *A*₂₂ + ... + *A*_{2j}; where *i* and *j* are numbers of individual deformed areas on each surface, thus *A*₁ and *A*₂ must

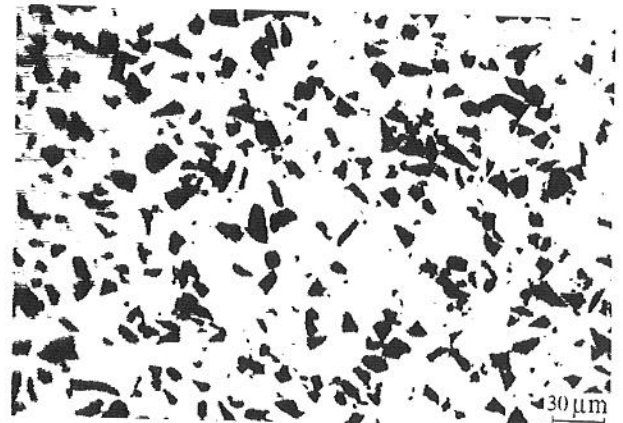


Fig. 1. Particle distribution in 20% Al₂O₃ aluminum composite with an average particle diameter of 8.8 μm.

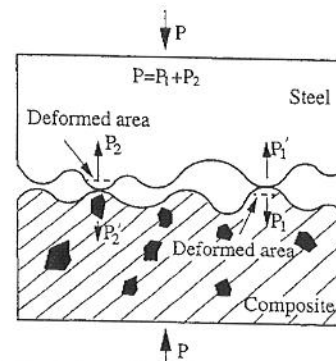


Fig. 2. Schematic illustration of the individual deformation area on steel and composite.

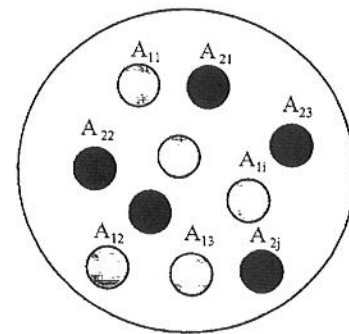


Fig. 3. Schematic illustration of the real contact area, plastically deformed and non-deformed, on the composite pin surface.

satisfy *A*₁ + *A*₂ = *A*_r, where *A*_r is the real contact area, which is much smaller than the nominal area of the pin surface. The hard asperities on the composite surface are those containing reinforced ceramic particles. From Fig. 2, the deformed areas on both surfaces are related to the real contact area *A*_r by

$$A_1 = (1 - P_p) A_r \tag{5}$$

and

$$A_2 = P_p A_r \tag{6}$$

where *P*_p is the probability or areal fraction of those areas whose hardness is higher than the other regions. For the present alumina particle reinforced aluminium composites,

we assume P_p equals to the particle volume fraction f_v , thus we have

$$A_1 = (1 - f_v)A_r \quad (7)$$

and

$$A_2 = f_v A_r \quad (8)$$

In plastic deformation, the load is proportional to the deformed area [16], and the total applied load P is therefore the summation of all individual loads which caused plastic deformations on each surface, i.e. $P_1 + P_2 = P$, where

$$P_1 = (1 - f_v)P \quad (9)$$

and

$$P_2 = f_v P \quad (10)$$

Substitution of Eqs. (9) and (10) into Eqs. (2) and (3) leads to

$$V_1 = \frac{K_1 PL}{H_1} (1 - f_v) \quad (11)$$

and

$$V_2 = K_2 \frac{PL}{H_2} f_v \quad (12)$$

The system volumetric wear is therefore

$$V = K_1 \frac{PL}{H_1} \left[(1 - f_v) + \frac{K_2 H_1}{K_1 H_2} f_v \right] \quad (13)$$

Alternatively, the specific wear rate is

$$w_s = \frac{V}{PL} = \frac{K_1}{H_1} (1 - f_v) + \frac{K_2}{H_2} f_v \quad (14)$$

Eq. (13) shows that the system wear is proportional to the total applied load and sliding distance, and is a function of the relative hardness of the rubbing materials and particle volume fraction of the composite.

3. Experimental verification

Pin-on-disk tests in a system of Al_2O_3 particle-reinforced 6061 Al composites (pin) sliding against carbon steels (disks) were conducted in a Plint-Cameron wear testing machine to examine the validity of the model. The composites used contained 10% (4.5 μm) and 20% (8.8 μm) angular Al_2O_3 -Al particles. A similar test using unreinforced 6061 Al alloy was also carried out for comparison. Two types of steel (AISI 1030 and AISI 4140) were used as counterpart surfaces. The tests were at a sliding speed of 1 m s^{-1} and an applied load of 100 N, under dry sliding condition at room temperature and 70% relative humidity. The microhardness values of the composites and steels are listed in Table 1. Atomic force microscopy was used to examine the worn surface. A real roughness profile after 1000 m sliding distance

Table 1
Microhardness of the tested materials (N mm^{-2})

Material	6061 Al	10% Al_2O_3	20% Al_2O_3	AISI 1030	AISI 4140
H_v	1176	1274	1421	1862	4410

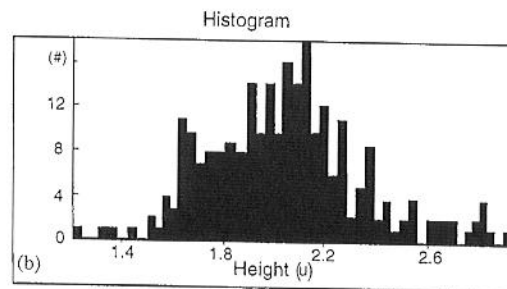
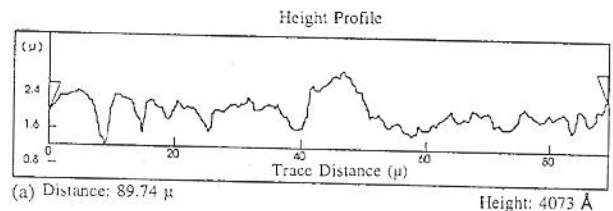


Fig. 4. (a) Real surface profile and (b) distribution of asperity heights, in steady wear obtained by an atomic force microscope.

Table 2
Specific wear rate of pins ($\text{mm}^3 \text{mN}^{-1}$) with soft and hard steel disks

Counterpart	Against AISI 1030	Against AISI 4140
Wear of 6061 Al alloy	0.0088	0.0092
Wear of 10% Al_2O_3 -Al	0.0072	0.0080
Wear of 20% Al_2O_3 -Al	0.0050	0.0056

Table 3
Specific wear rate of steels ($\text{mm}^3 \text{mN}^{-1}$) with different rubbing pairs

Counterpart	6061 Al alloy	10% Al_2O_3 -Al	20% Al_2O_3 -Al
AISI 4140 wear	0.0	0.0028	0.0062
AISI 1030 wear	0.0	0.0048	0.0137

is shown in Fig. 4(a) and a typical Gaussian distribution of asperity heights shown in Fig. 4(b). The wear results on the composites and steels are listed in Tables 2 and 3. The specific wear rates of both steels (AISI 1030) and composites are plotted against the particle volume fraction f_v in Fig. 5. As can be seen, with increasing f_v , the wear rate of the composites decreases while that of the steel increases. This is consistent with the early study by Wang and Rack [5], which explained the effect of the whisker volume fraction (f_w) and the relative hardness on the wear rate of steel in a SiC_w -Al/steel system. The difference between the whiskers and particles in the composite is that whiskers have to be clustered to form hard asperities while individual particle may form a hard asperity.

If these experimental data are used to determine the factors K_1 and K_2 in Eqs. (11) and (12), $K_1 = 0.96$, and $K_2 = 11.10$

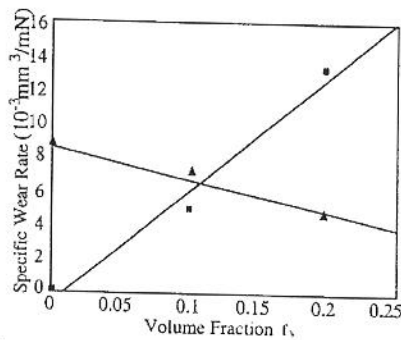


Fig. 5. Experimental results on the specific wear rate of steel disk (■) and MMC pin materials (▲) and best fit straight lines.

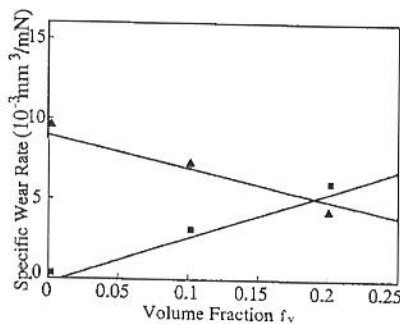


Fig. 6. Comparison of model predictions (—) and experimental results on the specific wear rates of AISI4140 steel disk (■) and MMC pin materials (▲).

are obtained. The predictions using Eqs. (11) and (12) on the wear of the same composites and AISI 4140 steel are shown in Fig. 6 together with the experimental results. Such a linear relationship between the steady wear rate and f_v was also found using aluminum–silicon alloy (A356) reinforced with 10% and 20% SiC ($9 \mu\text{m}$) particles when sliding at 0.8 m s^{-1} at a load of 98 N [1], which confirmed the applicability of the present model. However, it is admitted that the range of experimental data to test the model as presented in this work is far too limited. Much further work will be needed to demonstrate the general validity of the proposed steady wear model for metal matrix composites.

It is clear that the proposed model also has several limitations, i.e. the effect of particle size is not included and there should be no wear mechanism transitions. From previous studies, the range of particle appears to be limited to between 4 and $20 \mu\text{m}$ and the model is only applicable to particle volume fractions (f_v) between 0 and 30%. Composites with more than 30% particle volume fraction would become so brittle that the particle fracture effect on wear of the composite will play an important role. Moreover, the proposed model is only applicable to the case of steady wear, in which the *adhesive wear mechanism* is predominant. Other wear mechanisms such as oxidative and abrasive wear are excluded in this model.

4. Conclusion

Based on the analysis of asperity contact, a model on the steady wear of a steel disk being slid on by a pin of an MMC reinforced with ceramic particles is developed. The model, verified by some limited experiments, does show that the wear of each counterpart surface is influenced by the applied load, surface roughness, hardness and the particle volume fraction in the MMCs. The present work provides a theoretical basis to optimize wear resistance of metal matrix composites and rubbing materials.

Acknowledgements

The authors wish to thank Comalco Research Centre in Thomastown, Victoria for supplying the metal matrix composites for testing. The Electron Microscope Unit of Sydney University has provided access to its facilities. Z.F. Zhang was supported by an EMSS scholarship when this work was conducted. Support by the Australian Research Council on this project is much appreciated.

References

- [1] A.T. Alpas, H. Hu, J. Zhang, Plastic deformation and damage accumulation below the worn surfaces, *Wear* 162–164 (1993) 188–195.
- [2] J. Zhang, A.T. Alpas, Wear regimes and transitions in Al_2O_3 particulate-reinforced aluminum alloys, *Mater. Sci. Eng. A161* (1993) 273–284.
- [3] A. Wang, H. Rack, Transition wear behavior of SiC–particulate and SiC–whisker-reinforced 7091 Al metal matrix composites, *Mater. Sci. Eng. A147* (1991) 211–224.
- [4] A. Wang, H. Rack, Dry sliding wear in 2124 Al–SiC_w/17-4Ph stainless steel systems, *Wear* 147 (1991) 355–374.
- [5] A. Wang, H. Rack, A statistical model for sliding wear of metals in metal/composite systems, *Acta Metall. Mater.* 40 (9) (1992) 2301–2305.
- [6] N. Axen, S. Jacobson, A model for the abrasive wear resistance of multiphase materials, *Wear* 174 (1994) 187–199.
- [7] Z.F. Zhang, L.C. Zhang, Y.W. Mai, Wear of ceramic particle reinforced metal matrix composites. Part I: Wear mechanisms, *J. Mater. Sci.* 30 (8) (1995) 1961–1966.
- [8] J.F. Archard, Contact and rubbing of flat surfaces, *J. Appl. Phys.* 14 (1953) 981–988.
- [9] M. Khrushchov, Principle of abrasive wear, *Wear* 28 (1974) 69–88.
- [10] R. Holm, *Electric Contacts*, Almqvist and Wiksell, Uppsala, 1946.
- [11] E. Rabinowicz, *Friction and Wear of Materials*, Wiley, New York, 1965.
- [12] E.F. Finkin, An explanation of the wear of metals, *Wear* 47 (1978) 107–117.
- [13] J. Halling, A contribution to the theory of mechanical wear, *Wear* 34 (1975) 239–249.
- [14] J.A. Greenwood, J.B. Williamson, Contact of nominally flat surfaces, *Proc. R. Soc. London, Ser. A* 295 (1966) 300–319.
- [15] N.P. Suh, An overview of the delamination theory of wear, *Wear* 44 (1977) 1–16.
- [16] A. Wang, I.M. Hutchings, The number of particle contacts in two body abrasive wear of metals by coated abrasive papers, *Wear* 129 (1989) 23–35.